

Presentation of a novel model of chitosan- polyethylene oxide-nanohydroxyapatite nanofibers together with bone marrow stromal cells to repair and improve minor bone defects

Asgar Emamgholi ^{1, 4}, Mohsen Rahimi ^{2*}, Gholamreza Kaka ¹, Seyed Homayoon Sadraie ³, Saleh Najafi ⁴

¹ Neuroscience Research Center, Baqiyatallah University of Medical Science, Tehran, Iran

² Department of Parasitology and Mycology, School of Medicine, Baqiyatallah University of Medical Science, Tehran, Iran

³ Department of Anatomy, School of Medicine, Baqiyatallah University of Medical Science, Tehran, Iran

⁴ Microbial Biotechnology, Faculty of Science, Payame Noor University, Unit of Tehran Center, Tehran, Iran

ARTICLE INFO

Article type:

Original article

Article history:

Received: Mar 3, 2015

Accepted: Jul 7, 2015

Keywords:

BMSCs
Chitosan
Nanofibers
Scaffolds

ABSTRACT

Objective(s): Various methods for repairing bone defects are presented. Cell therapy is one of these methods. Bone marrow stromal cells (BMSCs) seem to be suitable for this purpose. On the other hand, lots of biomaterials are used to improve and repair the defect in the body, so in this study we tried to produce a similar structure to the bone by the chitosan and hydroxyapatite.

Materials and Methods: In this study, the solution of chitosan-nanohydroxyapatite-polyethylene oxide (PEO) Nanofibers was produced by electrospinning method, and then the BMSCs were cultured on this solution. A piece of chitosan-nanohydroxyapatite Nanofibers with BMSCs was placed in a hole with the diameter of 1 mm at the distal epiphysis of the rat femur. Then the biomechanical and radiographic studies were performed.

Results: Biomechanical testing results showed that bone strength was significantly higher in the Nanofiber/BMSCs group in comparison with control group. Also the bone strength in nanofiber/BMSCs group was significant, but in nanofiber group was nearly significant. Radiographic studies also showed that the average amount of callus formation (radio opacity) in nanofiber and control group was not significantly different. The callus formation in nanofiber/BMSCs group was increased compared to the control group, and it was not significant in the nanofiber group.

Conclusion: Since chitosan-nanohydroxyapatite nanofibers with BMSCs increases the rate of bone repair, the obtained cell-nanoscaffold shell can be used in tissue engineering and cell therapy, especially for bone defects.

► Please cite this article as:

Emamgholi A, Rahimi M, Kaka GR, Sadraie SH, Najafi S. Presentation of a novel model of chitosan- polyethylene oxide-nanohydroxyapatite nanofibers together with bone marrow stromal cells to repair and improve minor bone defects. Iran J Basic Med Sci 2015; 18:887-893.

Introduction

One of the common disorders in bone defects is the slow and often incomplete bone healing. Following ageing and delayed fracture union, decreased bone mass density entails heavy costs for the person and the society. Numerous therapeutic methods have been presented to accelerate the process of bone healing. Cell therapy is one of these therapeutic methods. The cells used for this purpose should have properties including easy availability, quick extension in the culture medium, long survival and adaptation in the host tissue. The cells should also be immunologically inert (1). Regarding these characteristics, it seems that bone marrow stromal cells (BMSCs) are multi-talented and nondifferen-

tiated cells within the bone marrow, but tissues such as blood, embryo, dental pulp, and adipose tissue are also similar to these cells (2). The role of BMSCs in bone tissue engineering has been studied extensively, and they have been used as tissue-repairing cells (3, 4). In a study, application of BMSCs has stimulated bone growth after fracture (5). BMSCs are able to produce different types of growth factors and cytokines (6) and can be differentiated into pseudo-osteoblast cells (7). Accordingly, in clinics these cells are used to treat bone disorders and their resulting limitation of activity (8).

BMSCs are adherent cells and can properly grow and proliferate on a scaffold. There are many methods for developing a scaffold where electro-

*Corresponding author: Mohsen Rahimi. Department of Parasitology and Mycology, School of Medicine, Baqiyatallah University of Medical Science, Tehran, Iran. Tel/Fax: +98-21-22284043; email: Mohsen1Rahimi@yahoo.com

spinning is a routine and available method. In this method, the polymer of interest is exposed to a magnetic field and afterwards the process of nanofiber production begins by exerting a high voltage. Several types of polymers such as chitosan have been used so far in the process of electrospinning. Chitosan, a co-polymer consisting of N-acetyl-glucosamine and N-glucosamine units (9), is first discovered in 1859 (10). The enzymatic destructibility of chitosan together with its structural similarity with extracellular matrix has made this polymer very important in bone tissue healing (11-15). In this research, to synthesize a chitosan-based nanofiber, polyethylene oxide (PEO) was used to reduce the viscosity of chitosan along with hydroxy apatite because of its similarity with the bone tissue (16). Hydroxy apatite is a bioactive material widely used in restoration of bone. This material, with its great similarity to the mineral phase of the hard tissue of the body, is of the most important known bioceramic with great applications in the biomaterials science. Thermodynamically, hydroxy apatite is a ceramic based on calcium and phosphorous, and it is stable in the physiological pH and temperature of human body (17).

Based on aforementioned, in order to combine and perform these therapeutic interventions simultaneously, first it is required to synthesize the chitosan-nanohydroxyapatite nanofiber using electrospinning and then cultivate the stromal bone cells on this nanofiber. This structure was then used to be evaluated on the bone defect and applied as a cell-scaffold cover to heal the bone fractures.

Materials and Methods

Materials

Chitosan with an average molecular weight of 109 kD and with 85% deacetylation was supplied by Sigma Co. PEO (Mw=900 kD), nanohydroxy apatite with mean diameter of 150 nm, mouse primary antibody of monoclonal antibody anti-CD44, anti-CD45 and anti-fibronectin and the secary anti-mouse antibody of avidin-biotin containing HRP (Horseradish peroxidase) as well as DAB (3,3'-Diaminobenzidine) dye were obtained from Sigma. The α -MEM culture medium, acetic acid (glacial), gelatin powder, trypsin 0.25%, ethylenediaminetetraacetic acid (EDTA) 0.04%, detectors and dyes and Triton X-100 was provided by Merck, Germany. Wistar rats were provided by animal laboratory in neuroscience center of Baqiyatallah Research Center. After the surgical operation, the animals were divided into three equal groups randomly. Control, Nanofiber and Nanofiber/BMSCs groups.

Electrospinning

Initially, 2% weight-volume solution of chitosan and 3% weight-volume solution of PEO were

separately dissolved in 0.5 M acetic acid. These solutions were then mixed with a 9 to 1 volume-volume ratio (Chitosan-PEO), followed by electrospinning to obtain the optimal conditions. In order for the placement of nanohydroxy apatite within the nanofiber structure, 0.2 g of nanohydroxy apatite powder was added to 5 ml of the chitosan-PEO solution prepared in the previous stage, and the solution was mixed for 5 hr resulting in a milky solution. Then the electrospinning was repeated.

To this end, 0.5 ml of the synthesized solutions poured into a 2-ml syringe with a needle tip of 0.5 mm. They were then placed in an electrospinning instrument (FANAVARSAN, Iran) between two opposite poles, and the process of nanofiber synthesis started by exerting a potential difference from 18 to 22 KV. A scanning electron microscope (SEM) made by LEO Co. (VP 1455, England) confirmed the shape and the mean diameter of the nanofiber made through electrospinning. To determine the mean thickness of nanofibers, 5 SEM images were taken from different points, and from each image, 10 locations of nanofibers were selected and the average thickness was calculated. The chitosan- PEO -nanohydroxyapatite nanofiber were characterized by Fourier transform infrared spectroscopy (FTIR) (Perkin Elmer).

Extraction of BMSCs and cultivating on nanofibers

Through following the principles required to work with laboratory animals, BMSCs were extracted from the femur of adult Wistar rats (6 to 8 weeks old). After anesthetizing the animals by mixture of Ketamine (50 mg/kg) and Xylazine (5mg/kg) using Betadine surgical solution and 70% ethanol, the posterior and dorsal limbs of the animal were thoroughly sterilized (18). The bones were then cut in half, and the bone marrow was aspirated through the bone canal using a 5-ml syringe containing 1 ml of α -MEM culture medium. The contents of the syringe was poured into a 6-cm plate containing the medium and fetal bovine serum (FBS) 10% and was put into a CO₂ incubator (MMM, England). After 24 hr, the cellular culture medium was replaced with the fresh medium. Stromal cells attached to the flask floor remained and the floating blood cells were removed. When the density of cells attached to the flask floor reached 70 to 80%, the cells were passaged using Trypsin 0.25% and EDTA 0.04%. This was repeated up to three passages until the cells reached a similar morphology. A cellular suspension was then prepared and cultured on the nanofiber. For this purpose, using gelatin 1%, first the nanofiber was attached to the plate floor with a 0.5 cm diameter, and then sterilized using a 75% alcohol (16) and distilled-washed. After performing viability test using Trepan blue, from the cellular suspension, 5*10³ cells were added to each of the cellular culture plates and were then placed into a 5% CO₂ incubator at 37 °C.

Table 1. Evaluation and grading of bone callus

The degree of bone callus	Grade or score
Devoid of callus	Zero
Very poor callus	One
Poor callus	Two
Medium callus	Three
Good callus	Four
Very good callus	Five

Immunocytochemistry

After four days from cultivation of cells on nanofibers, in order to determine the purity of stromal cells, first BMSCs were fixed on a coverslip using paraformaldehyde 4% for 30 min. Cell cleansing with phosphate-buffered saline (PBS) was performed three times and each time for 5 min. The samples were exposed to the mixture of 10% Goat serum and 0.3% Triton X-100 for 1 hr. After dilution (1:100), the CD44 and fibronectin primary antibodies, which both were murine, were poured onto the cells separately. In order to prevent antibody drying, the samples were covered by a piece of parafilm and were then incubated at 4°C in a humid Petri dish for one night. After cleansing with PBS, the coverslips were exposed to the fresh solution of H₂O₂ 10% for 30 min. Next, cleansing with PBS was performed three times. They were then exposed to anti-murine secondary antibodies (1:200) of avidin-biotin for 2 hr. This was followed by exposure to DAB chromogene solution that generates brown sediment (for 10 min). Cleansing with PBS was re-performed, and the samples were investigated using an invert microscope.

Making a bone defect

In this research, 21 male adult Wistar rats (with an approximate weight of 200-250 g) were used. To create a bone defect in the animal, the outer surface of the animal thigh was shaved and the area was cleansed with betadine. Using a fully sterile method, the area in its right leg was cut 2 cm long. After pushing aside superficial muscles and deep fasciae, the femur was then exposed. Using a drill with a 1 mm diameter, a hole was created transcortically in epiphysis distal region of the femur. After the surgical operation, the animals were divided into three equal groups randomly. Control, was a group that received no treatments. Nanofiber was a group in which a piece of chitosan-nanohydroxyapatite nanofiber was dragged with a 25-mm² area at the defect site. Nanofiber/BMSCs, was a group that a piece of chitosan-nanohydroxyapatite nanofiber together with 5*10⁴ BMSCs was dragged with a 25-mm² area at the defect site.

Collecting specimens from the animals

The mice were slaughtered 28 days after the first operation using high-dose chloroform. The bone was then removed and investigated biomechanically and radiographically.

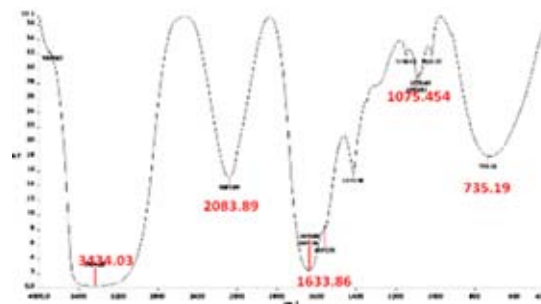


Figure 1. Normalized transmission FTIR spectra recorded at room temperature in the (OH), (CO₃²⁻), (NO₃⁻) and (PO₄³⁻) region for chitosan- PEO -Nanohydroxyapatite nanofiber mixture

Biomechanical test of bones

The bone biomechanical strength was examined using three point bending test by Zwick 2.5 (Germany) device. The femur bone was put on the holder legs from both ends and the force perpendicular to the longitudinal axis of bone was exerted by the system operator in the posterior-anterior direction. The actuator speed was 5 mm/min and the pressure was further increased on the bone until its fracture. The maximum mechanical strength of the bone (F_{max}) was calculated in terms of Newton by drawing the force-length variation curve.

Radiographic examination

The radiographic investigation of the right-leg femur samples was carried out by a Senographe 600T Senix H.F device with a radiation dose of 22 KV at 9 mas. Radiography was performed at the posterior-anterior and lateral views on mammographic films. The radiographic images encoded by orthopedic and radiologic specialists were evaluated and scored in terms of density and bone callus using the modified method of Madsen and Hukkhanen (19) (Table 1).

Statistical analysis

All values have been presented after three times repetitions of the experiment in terms of Mean±SEM. The information obtained from one-way analysis of variance (one-way ANOVA) and Tukey test were compared and the significance level was considered at P-value<0.05.

Results

FTIR

Figure 1 shows the FTIR spectra obtained for chitosan- PEO -Nanohydroxyapatite nanofiber mixture. The absorption peak observed at 3434.03 cm⁻¹ is typical of the vibration stretching of the hydroxyl (OH) group. The strong peak observed at 2083.89 cm⁻¹ is the vibration stretching of the carbonate (CO₃²⁻) band. As well, the strong peak observed at 1633.86 cm⁻¹ is typical of the vibration stretching of the nitrate (NO₃⁻) group, and the peak observed at 735.19 cm⁻¹ is the vibration stretching of the phosphate (PO₄³⁻) band.

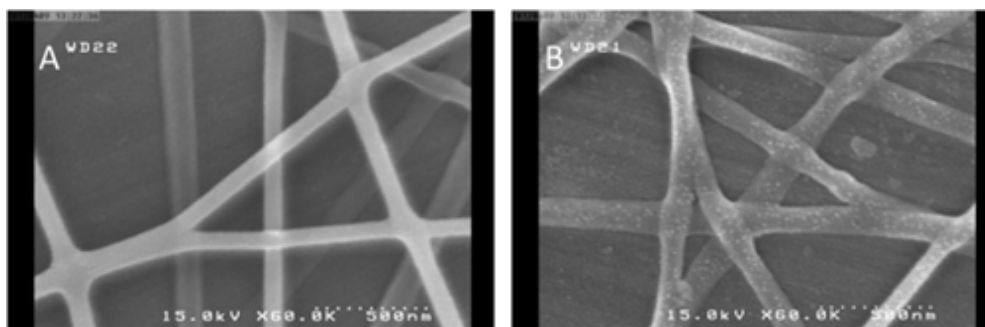


Figure 2. SEM images of chitosan nanofiber (A) and chitosan-nanohydroxyapatite nanofiber (B)

Electrospinning

According to SEM images, the nanofiber was fabricated homogeneously with no nodes during the electrospinning process. The mean diameter of nanofibers was 100 nm. The nanofiber devoid of nanohydroxyapatite (Figure 2, A) had a better quality than the nanofiber containing nanohydroxyapatite (Figure 2B).

Determination of the cell viability by the Tripin blue

Based on viability test, in which the live cells were counted 24 hr after the third passage, the cell viability was 91%.

Immunocytochemistry test

Fibronectin, CD44, and CD45 antibodies were used to prove the stromaticity of BMSCs and to determine their purities. Figure 3 demonstrates the cells with a cytoplasm containing fibronectin brown fibers (white arrows). To determine the percentage of positive cells, the nucleus of cells was changed into violet by hematoxylin, where $92.75 \pm 3.86\%$ of cells reacted with anti-fibronectin and $94.3 \pm 4.66\%$ of cells reacted with CD44. At this stage, the CD45 antibody specific to hematopoietic cells was expressed in only $4.5 \pm 2.18\%$ of the cells (Figure 3).

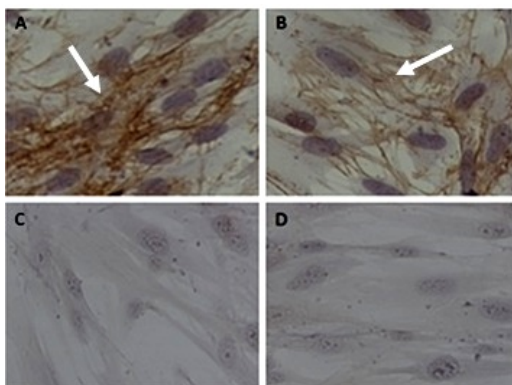


Figure 3. The microscopic images of stromatic cells after immunocytochemistry assay with a 400-X magnification. Images (A), (B), (C), and (D) are related to CD44 antibody, fibronectin antibody, CD45 antibody, and negative control of BMSC cells, respectively four days after cultivation of cells onto the nanofiber from the third passage. A and B are seen as brown (white arrows) due to the presence of CD44 markers and fibronectin

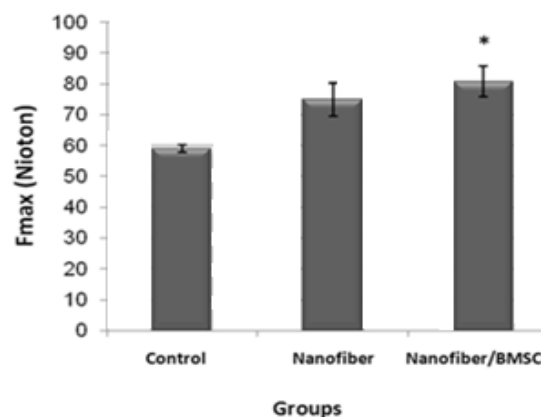


Diagram 1. The mean F_{max} for different groups four weeks after cell grafting; *Significant difference with the control group

Biomechanical test results

The biomechanical test results for the femur bones four weeks after BMSCs and nanofiber grafting in groups indicated that the mean F_{max} against flexural strength was 59.1 ± 1.15 in the control group, 75.0 ± 5.50 in the nanofiber group, and 80.8 ± 4.96 in the nanofiber/BMSCs group. According to the statistical tests, the mean F_{max} had significant increase in the nanofiber and nanofiber/BMSCs groups compared to the nontrol group. This elevation was significant in the nanofiber/BMSCs group (P -value<0.05) and close to significant (P -value= 0.09) in the nanofiber group. There was no significant difference between the nanofiber and nanofiber/BMSCs groups in terms of maximum bone strength (Diagram 1).

Radiography

The radiographic results indicated that the mean level of bone callus formation (the radio-opacity of control group was 2.1 ± 0.136 and the nanofiber group was 2.18 ± 0.121) did not have a significant difference. The level of bone callus formation in the nanofiber/BMSCs group was 2.6 ± 0.32 , with an elevated level compared with the nanofiber group. However, this increase was not significant (Diagram 2).



Figure 4. Images obtained from the impact of X-ray on the site of bone callus formation. The arrows show the site of bone callus in animals for (A) Control, (B) Nanofiber, and (C) Nanofiber/BMSCs groups. As can be observed from the images, the degree of bone callus has increased in (C) and (B) compared to (A), where it is greater in (C)

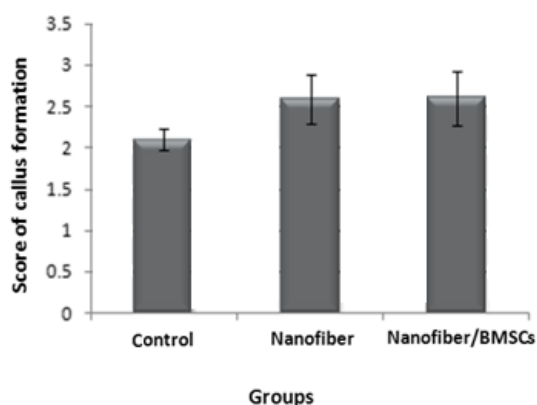


Diagram 2. Comparison of the mean bone callus formation among the groups four weeks after grafting

The images obtained from callus formation at the site of defect can be observed in Figure 4 for different groups. Callus formation at the injury site was greater and clearer in nanofiber and nanofiber/BMSCs groups compared with the control group. In addition, more callus formation by the femur was observed in the nanofiber/BMSCs group compared with the nanofiber group.

Discussion

In this research, for bone tissue engineering, nanohydroxyapatite was added to the composite to make it similar to the natural tissue. Hydroxyapatite is a bioactive material and thereby has unique biological characteristics. This property enables the hydroxyapatite to directly produce bonds with body cells that induce bone growth. Studies have shown that the reason of this phenomenon is related to a protein called Osteocalcin that can attach to hydroxyapatite. This protein plays the role of a signaler for osteoblast cells (bone-generating cells) (20). Zhang *et al* (2008) developed a scaffold made from nanohydroxyapatite and chitosan nanofiber using co-deposition method (21).

In this study, PEO due to its biocompatibility was used to produce the desired nanofiber (16). The

results of research in which polyvinyl alcohol (PVA) (22) and polycaprolactone (PCL) (23) have been used to produce the Nanofiber were also similar to our findings. The results showed that chitosan itself has lower electrospinning ability and cannot synthesize nanofibers. FTIR data showed that the reason for better formation of PEO chitosan nanofiber is the formation of hydrogen bonds between these two polymers. Bhattaraia *et al* (2005) electrospun different percentages of composite solutions of chitosan and PEO and indicated that the chitosan-PEO nanofibers with 90:10 ratio maintained their structure well in water and result in improved adherence of chondrocyte and osteoblast cells (16). Our results were very similar to their findings in terms of nanofiber synthesis and cell culture.

In the present research, to determine the purity of stromatic cells due to the presence of glycoprotein fibronectin in mesenchymal-originated cells, BMSCs were stained against this glycoprotein using the immunocytochemistry method. High expression of fibronectin in the cells confirmed that they are stem cells (24). For confirmation of the purity of BMSCs, CD44 antibodies were used and the results indicated a high percentage of positive cells for the fibronectin antibody. This results has also been observed by others regarding mesenchymal stem cells (25). Through application of anti-fibronectin antibody and the mRNA expression of Oct-4 gene, Lamoury *et al* cultured BMSCs of animals and humans in two separate media and verified that they were stem cells (26).

In this research, radiographic results obtained from the site of minimal bone defect in femur four weeks after nanofiber grafting without cells and nanofiber plus BMSCs revealed that at the site of bone injury, the amount of bone callus (radio-opacity) was increased insignificantly in both states compared with the control group. In agreement with our research, Stockman *et al* developed a single-layer defect within the cortical region in the pig skull and performed autologous grafting of BMSCs together

with collagen scaffolds. In that study, the groups consisted of a control group for which collagen was embedded alone and experimental group. For radiography, the skull capsule was removed and exposed to X-ray to determine the degree of defect healing. Thirty days after grafting, no difference was observed between the control and experimental groups, although their results were different from our findings in the 30th day, because these results revealed a relatively insignificant increase in both groups compared with the control group. However, Stockman indicated that at the 60th and 90th days, the rate and degree of bone mineralization in the BMSCs graft group were significantly greater than the control group (27). In another research, grafting of BMSCs with TCP (Tri-calcium phosphate) scaffold was performed in goats with osteoporosis that had cylindrical defects in condyle of the femur bone. The animals were investigated radiographically after 16 weeks. In the X-ray analysis, formation of the new bone and its healing percentage were determined as radio-opaque volume. In group A that the defect site had no grafts, the radio-opacity was minimized and there were almost no bones formed at the site of defect. In group B that the defect was filled with TCP, no evident restoration was observed at the defect site and only in some regions related to the defect margin; radio-opaque region was observed. In group C in which the stem cells were grafted with TCP, the bone formation was significant and was well integrated with the tissue around the defect. Therefore, the factor or percentage of new bone in the cell-therapy group was increased more than other groups (28).

Our result of biomechanical test demonstrated that the mean bone strength (F_{max}) had a significant increase in the nanofiber/BMSCs group compared with the control group, while it was insignificant in the nanofiber group in comparison with the control group. The results of a study in which BMSCs grafting together with collagen Type 1 had been used at the site of bone defect in the femur of mice suffering from osteogenic defects, revealed that the biomechanical test of this group compared with the group receiving only collagen Type 1 or only PBS had a greater mechanical strength. It is argued that differentiation of BMSCs to osteoblast is followed by bone formation in *in vivo*. On the other hand, in addition to BMSCs, endogenic cells also are applicable for restoration. This mechanism is realized in two ways: one through the production of androgenic cells and the other through the factors of TGF- β proteins family such as Bone morphogenetic proteins (BMPs) and vascular endothelial growth factors (VEGF) (29).

Conclusion

It can be concluded that as BMSCs could easily grow and proliferate on the chitosan-nanohydroxyapatite nanofibers and could keep their stemming quality, an

appropriate cover of cell-nanoscaffolds was obtained to be applied in fractures and defects of bones. This was further supported by elevation of bone healing rate through grafting chitosan-nanohydroxyapatite nanofibers with BMSCs.

Acknowledgment

The authors thank Dr Tahereh Mohammadzadeh and Dr Minoos Sadri for their kindly helps, Tehran, Iran.

References

- Jorgensen CH. Mesenchymal stem cells in arthritis: role of bone marrow microenvironment. *Arthritis Res Ther* 2010; 12:135.
- Valtieri M, Sorrentino A. The mesenchymal stromal cell contribution to homeostasis. *J Cell Physiol* 2008; 217:296-300.
- Bergfeld SA, DeClerck YA. Bone marrow-derived mesenchymal stem cells and the tumor micro-environment. *Cancer Metastasis Rev* 2010; 29:249-261.
- Hideaki K, Hideki A, Arinobu T. Bone marrow stromal cells (bone marrow-derived multipotent mesenchymal stromal cells) for bone tissue engineering: Basic science to clinical translation. *Int J Biochem Cell Biol* 2011; 43:286-289.
- Salasznyk RM, Williams WA, Boskey A, Batorsky A, Plopper GE. Adhesion to vitronectin and collagen I promotes osteogenic differentiation of human mesenchymal stem cells. *J Biomed Biotechnol* 2004; 1:24-34.
- Araki T, Nagarajan R, Milbrandt J. Identification of genes induced in peripheral nerve after injury. *J Biol Chem* 2001; 276:34131-34141.
- Anita M, Ranieri C, Rodolfo Q. Clonal mesenchymal progenitors from human bone marrow differentiate *in vitro* according to a hierarchical model. *J Cell Sci* 2000; 113: 1161-1166.
- Tohill M, Mantovani C, Wiberg M, Terenghi G. Rat bone marrow mesenchymal stem cells express glial markers and stimulate nerve regeneration. *Neurosci Lett* 2004; 362:200-203.
- Homayonia H, Hosseini Ravandia SA, Valizadehb M. Electrospinning of chitosan nanofibers: processing optimization. *Carbohydr Polym* 2009; 77:656-661.
- Khora E, Yong Lim L. Implantable applications of chitin and Chitosan. *Biomaterials* 2003; 24:2339-2349.
- Kumar MNVR. A review of chitin and Chitosan applications. *React Funct Polym* 2000; 46:1-27.
- Yogi K, Michibayashi N, Kurikawa N, Nakashima Y, Mizoguchi T, Harada A, *et al*. Effectiveness of fructose-modified Chitosan as a scaffold for hepatocyte attachment. *Biol Pharm Bull* 1997; 20:1290-1294.
- Zhang Y, Zhang MQ. Calcium phosphate/Chitosan composite scaffolds for controlled *in vitro* antibiotic drug release. *J Biomed Mater Res* 2002; 62:378-386.
- Zhang Y, Zhang MQ. Three-dimensional macroporous calcium phosphate bioceramics with nested Chitosan sponges for load-bearing bone implants. *J Biomed Mater Res* 2002; 61: 1-8.
- Zhang Y, Zhang MQ. Synthesis and characterization of macroporous Chitosan/calcium phosphate composite scaffolds for tissue engineering. *J Biomed Mater Res* 2001; 55:304-312.

16. Bhattaraia N, Edmondson D, Veiseha O, Matsen FA, Zhang M. Electrospun chitosan-based nanofibers and their cellular compatibility. *Biomaterials* 2005; 26:6176–6184.
17. Fouda MFA, Nemat A, Gawish A, Baiuomy AR. Does the coating of titanium implants by hydroxyapatite affect the elaboration of free radicals. *An Experimental Study. Austr J Basic Appl Sci* 2009; 3:1122-1129.
18. Seung Y. The survival and migration pattern of the bone marrow stromal cells after intracerebral transplantation in rats. *J Korean Neurosurg* 2004; 400-404.
19. Madsen JE, Hukkhanen M. Fracture healing and callus innervations after peripheral nerve resection in rats. *Clin Orthopaed Relat Res* 1998; 351:230-240.
20. Boskey AL, Wians FH, Hauschka PV. The effect of osteocalcin on *in vitro* lipid-induced hydroxyapatite formation and seeded hydroxyapatite growth. *Calcif Tissue Int* 1985; 37:57-62.
21. Yanzhong ZH, Jayarama R, Adel E, Seeram R, Bo SU, Teck L. Electrospun biomimetic nanocomposite nanofibers of hydroxyapatite/Chitosan for bone tissue engineering. *Biomaterials* 2008; 29:4314-4322.
22. Faheem A, Naseer A, Muzafar A, Soo Jin P, Dae Kwang P and Hak Y. Synthesis of Polyvinyl alcohol (PVA) nanofibers Incorporating Hydroxyapatite nanoparticles as Future Implant Materials. 2010; 18: 59-66.
23. Han L, Anthony A, Montserrat C, Megan C, James B, Salim C, *et al.* Composite tissue engineering on polycaprolactone nanofiber scaffolds. *Ann Plast Surg* 2009; 62:505-512.
24. Zhao LR, Duan WM, Reyes M, Keene CD, Verfaillie CM, Low WC. Human bone marrow stem cells exhibit neural phenotypes and ameliorate neurological deficits after grafting into the ischemic brain of rats. *Exp Neurol* 2002; 174:11-20.
25. Bossolasco P, Cova L, Calzarossa C, Rimoldi SG, Borsotti C, Delilieri GL, *et al.* Neuro-glial differentiation of human bone marrow stem cells *in vitro*. *Exp Neurol* 2005; 193:312-325.
26. Lamoury FM, Croitoru-Lamoury J, Brew BJ. Undifferentiated mouse mesenchymal stem cells spontaneously express neural and stem cell markers Oct-4 and Rex-1. *Cytotherapy* 2006; 210:228-242.
27. Stockmann P, Wilmowsky J, Nkenke V, Felszeghy C, Friedrich E, *et al.* Guided bone regeneration in pig calvarial bone defects using autologous mesenchymal stem/progenitor cells-a comparison of different tissue sources. *J Craniomaxillofac Sur* 2012; 40:310-320.
28. Cao L, Liu G, Gan Y, Fan Q, Yang F, Zhang X, *et al.* The use of autologous enriched bone marrow MSCs to enhance osteoporotic bone defect repair in long-term estrogen deficient goats. *Biomaterials* 2012; 33:5076-5084.
29. Li F, Wang X, Niyibizi C. Bone marrow stromal cells contribute to bone formation following infusion into femoral cavities of a mouse model of osteogenesis imperfecta. *Bone* 2010; 47:546-555.